BJRS

BRAZILIAN JOURNAL
OF
RADIATION SCIENCES
10-02A (2022) 01-15

SBPR
Sociedade Brasileira de Proteção Radiológica

Structural and Morphological Characterization of the Chromium-doped β-Spodumene to Ceramic Pigment

Ferraz[a] R.F., Sousa[a] J.F., Lima[b] H.R.B.R., Oliveira[a], R.A.P.

[a] *Universidade Federal do Vale do São Francisco / Colegiado de Pós-graduação em Ciência dos Materiais, 48920-310, Juazeiro, Bahia, Brasil*

[b] *Instituto Federal de Sergipe / Colegiado de Física, 49400-000, Lagarto, Sergipe, Brasil*

E-mail address: ricardo.univasf@gmail.com

ABSTRACT

The structural and morphological properties of a novel chromium-doped β-spodumene based ceramic pigment were evaluated aiming to study its chemical and thermal stability in industrial applications. The pigment samples were synthesized by the proteic sol-gel method using gelatin as a ligand. X-ray diffraction (XRD) and scanning electron microscopy (SEM) were performed. Rietveld refinement of experimental diffractograms and average crystallites size by the Scherrer's method analysis were carried out. XRD results confirmed that the crystal structure of lattice corresponded to β-spodumene, and the Rietveld refinement indicated the absence of structural changes with doping up to 3% of chromium. Scherrer's method indicates that there are no trends changes in the average size of crystallites in the analyzed doping contents. SEM analysis indicated that there are no morphological changes in the chromium-doped particles. The present study concluded that structural or morphological alterations are not noticed for β-spodumene samples produced with chromium doping up to 3% by weight and that this pigment possibly preserves the chemical and thermal stability of pure β-spodumene. The absence of changes in these properties by doping with low chromium contents was attributed to possible substitutions of Al^{3+} by Cr^{3+} ions in the β-spodumene crystal lattice.

Keywords: **β-spodumene, ceramic pigment, proteic sol-gel method.**

ISSN: 2319-0612
DOI: https://10.15392/bjrs.v10i2A.1772
Submitted:2021-12-06
Accepted: 2022-04-06

1. INTRODUCTION

Spodumene ($LiAlSi_2O_6$) is an important mineral to lithium extraction and has been synthesized for several applications [1-5]. It also has been evaluated for solid-state dosimetry using optically stimulated luminescence (OSL) and thermoluminescence (TL) and has shown great potential use for high gamma radiation doses detection [5-10]. Among its most recent studied applications, the use in the production of industrial ceramic pigments stands out, due to its chemical and thermal stability and the possibility of incorporating chromophore ions in its structure of lattice by high-temperature synthesis [11].

Pigments can color materials from the dispersion of insoluble particles and their color occurs due to the action of a chromophore ion incorporated in the structure. Chromophore ions, usually transition metals, have a partially filled electronic envelope, enabling electronic transitions by interacting with visible radiation and can replace ions with similar properties (charge and radius) in the matrix [12]. For β-spodumene ceramic pigment, the occurrence of selective absorption was produced by the addition of Cr^{3+} ions into the structure. This absorption occurs in the 425 nm and 600 nm bands (violet and orange light), resulting in the complementary yellowish-green color [11].

The production of silicates and aluminosilicates-based pigments as raw materials has increased significantly, mainly due to its solid-phase reactions at relatively low temperatures [13] and the eco-friendly synthesis possibilities using highly available raw material or from waste [14,15]. Sol-gel method has been noteworthy to the synthesis of oxide ceramics, presenting advantages such as good homogeneity of metallic precursors and reduced synthesis temperatures compared to the solid-state reaction method, due to shorter diffusion path [16,17]. The proteic sol-gel method is an improved method of the traditional sol-gel, which replaces metal alkoxides with protein ligands, usually the hydrolyzed collagen, associated with inorganic precursors [18]. The formation of the gels is caused by hydrolysis and polycondensation reactions [19].

In this paper, the structural and morphological characteristic of synthetic chromium-doped β-spodumene based pigment were evaluated. This structure corresponds to the synthetic polymorph with the tetragonal unit cell, produced by a proteic sol-gel route. It was verified whether chemical and thermal stability are preserved with the addition of chromium dopant in this structure, enabling its application as a novel industrial ceramic pigment.

2. MATERIALS AND METHODS

The preparation of samples was based on Ferraz et al. [11], who first produced the chromium-doped β-spodumene ceramic pigment using the proteic sol-gel route and determined its optical behavior. The applied synthesis temperatures were based on the thermal analyzes determined by Lima et al. [10], who first synthesized pure β-spodumene by this method. The flowchart in Figure 1 summarizes the materials and methods used in this research.

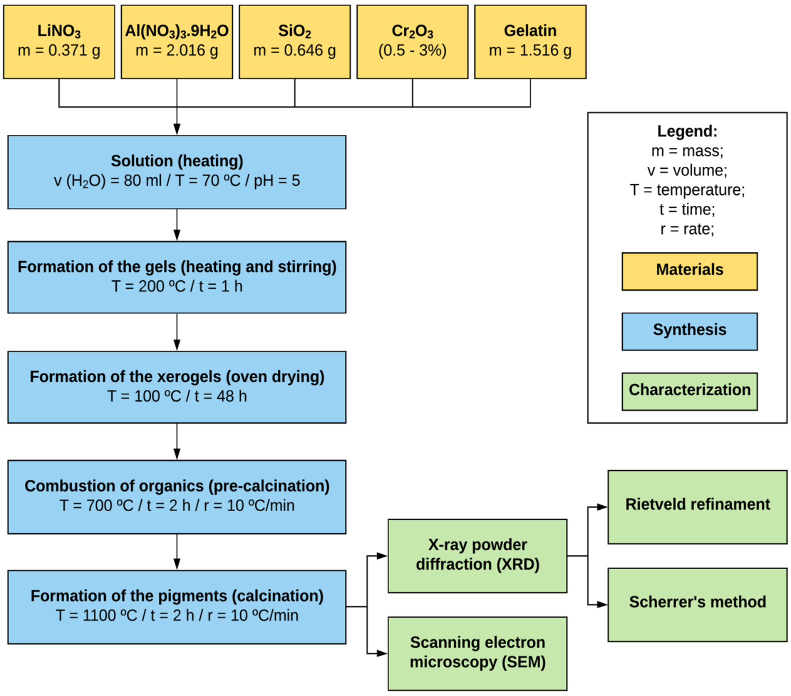

Figure 1: *Methodology flowchart: materials and synthesis and characterization techniques.*

2.1. Preparation of the samples

The reagents used were: $LiNO_3$ (Dinâmica®, 95% of purity), $Al(NO_3)_3.9H_2O$ (Dinâmica®, 98.5% of purity), SiO_2 (NEON, 98% of purity), Cr_2O_3 (NEON, 98% of purity), and gelatin powder (Royal®) as a proteic ligand. Initially, a solution was prepared to contain a ratio of 0.5 to 1 by weight of ligands to reagents. The proportions used for the production of 1g of β-spodumene per sample were: 0.341 g of $LiNO_3$, 2.016 g of $Al(NO_3)_3.9H_2O$, 0.646 g of SiO_2 and proportions relative to the total weight of the reagents of 0.5, 1, 1.5, 2, 2.5, and 3% of the dopant Cr_2O_3. The mass of gelatin used was 1.516 g per sample. The balanced chemical reaction is presented in Equation 1.

$$LiNO_3 + Al(NO_3)_3.9H_2O + 2SiO_2 \xrightarrow{T=1100\ ^{\circ}C} \beta - LiAlSi_2O_6 + 4HNO_3(gas) + 7H_2O(gas) \quad (1)$$

Initially, 80 ml of distilled water were heated to 70 ºC and the reagents and ligands were added in the specified proportions. This solution has an acidic character (pH = 5) due to the formation of nitric acid in an aqueous medium, which favors gelatin condensation reactions. The solutions were heated at 200 °C for 1 h with constant stirring to form the gels. The gels were dried in an oven at 100 ºC for 48 h to form xerogels. After crushing in a porcelain mortar and pestle (Figure 1a), the xerogels were subjected to pre-calcination in a boat-type alumina crucible at 700 °C for 2 h and a heating rate of 10 °C/min for complete combustion of the organic chains (Figure 1b). The samples were submitted to final calcination at 1100 ºC for 2 h at a heating rate of 10 ºC/min for the formation of the β-spodumene crystalline phase (Figure 1c). Cooling was applied slowly in a closed oven until reaching room temperature (25 ºC). Figure 2 illustrates the 3% chromium-doped β-spodumene sample, during the different stages of synthesis. The final pigments obtained have a yellowish-green color.

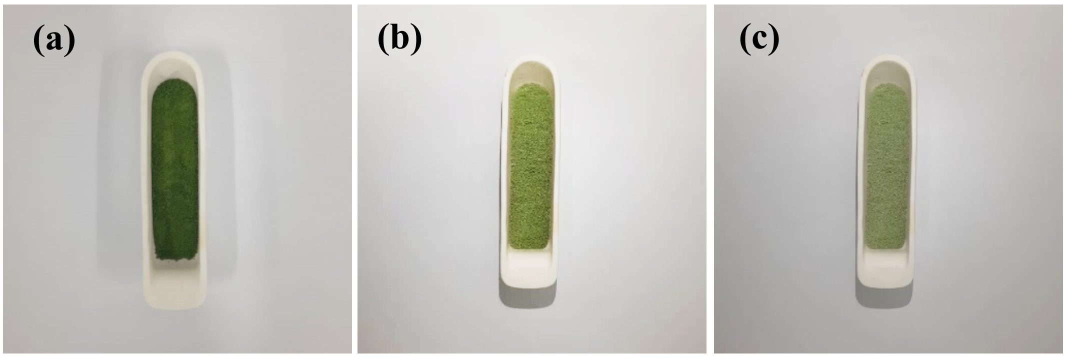

Figure 2: *3% chromium-doped β-spodumene pigment sample: (a) after drying the xerogel; (b) after pre-calcination / loss of organics; (c) after calcination / formation of the crystalline phase.*

2.2. Structural and morphological characterization

Measurements of X-ray diffraction (XRD) were taken with a powder diffractometer (Rigaku Miniflex), with Cu-K_α radiation ($\lambda = 1.5418$ Å), tube operating at 40 kV and 15 mA in the continuous mode with a speed of 10 °/min, steps of 0.02 ° and room temperature. Powder samples produced with different concentrations of the dopant and with particle sizes between 75 – 150 µm were analyzed. The experimental diffractograms obtained were compared with the theoretical patterns available in the PDF2 (Powder Diffraction File) crystallographic database from the positions and intensities of the Bragg crystalline peaks and the most probable references using the X'Pert HighScore Plus (PANalytical B. V.) software. The Rietveld refinement method [20] was provided to confirm quantitatively the occurrence of the β-spodumene phase for the samples produced, using the DBWSTools 2.4 program [21].

The size of crystallites (τ) was determined by the Scherrer's method (Equation 2) [22], which are obtained from the line broadening at half the maximum intensity (FWHM), or simply β, in radians, a dimensionless shape factor, with a value close to unity (K), the X-ray wavelength (λ) and the Bragg angle (θ). The values given are averages for the size of the crystallites obtained from the five highest intensity peaks.

$$\tau = \frac{k\,\lambda}{\beta\, cos\theta} \tag{2}$$

The Pseudo-Voigt function was used to fit the peak profiles of the identified crystalline phase. The Caglioti equation (Equation 3) was selected to correct the line broadening for the instrumental effects, where U, V and W are the half-width parameters obtained from the Rietveld refinement.

$$\beta = \sqrt{U\,tan^2\theta + V\,tan\theta + W} \tag{3}$$

Morphological analysis of the pigment particles was taken with a scanning electron microscope (SEM) Vega 3XM (Tescan) at accelerating voltage of 20 kV, equipped with secondary electrons detector. The specimen was mounted on a metal stub using a sticky carbon strip that increases conductivity. Gold coating was additionally applied for even more conductivity. The micrographs were performed at magnifications of 100, 500, and 1000 times in a low vacuum.

3. RESULTS AND DISCUSSION

3.1. Structural characterization

Figure 3 shows the X-ray powder diffractograms (XRPD's) obtained for the chromium-doped β-spodumene samples produced. The experimental patterns were compared to the ICSD 26817 reference pattern, which corresponds to the synthetic spodumene with a tetragonal crystalline structure [23]. All diffractograms showed identical crystalline structures and well-defined peaks, that are matched to the reference pattern, demonstrating that the synthesis was successful. No changes were noted in the diffractograms as the chromium content increased up to 3%.

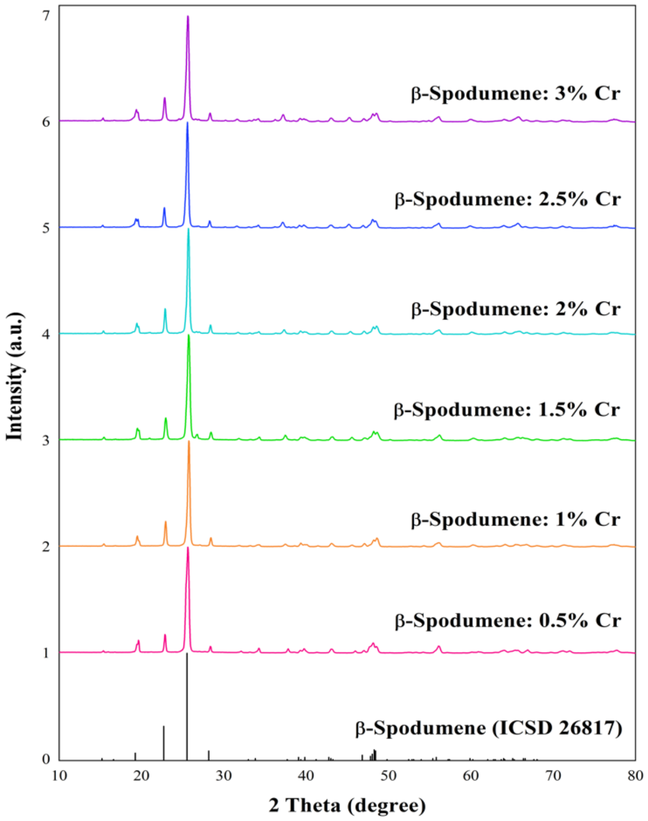

Figure 3: *Experimental XRPD's of chromium-doped β-spodumene pigment samples, and the reference pattern ICSD 26817.*

The crystalline structure for this β-spodumene phase is shown in Figure 4. This structure has a tetragonal crystal system having the space group $P4_32_12$. The crystallographic parameters are: a = b = 7.541 Å ≠ c = 9.156 Å; α = β = γ = 90º; volume = 520.67 × 10^6 pm^3; and density = 2.37 g/cm^3. The structure consists of a three-dimensional aluminosilicate framework and lithium atoms are stuffed in interstitial positions [23]. The presence of the Cr^{3+} dopant, at low levels presented in this research, does not cause the formation of a second phase, which is probably due to the substitution of Al^{3+} ions in the crystal structure, owing to their similar chemical properties (charge and radius).

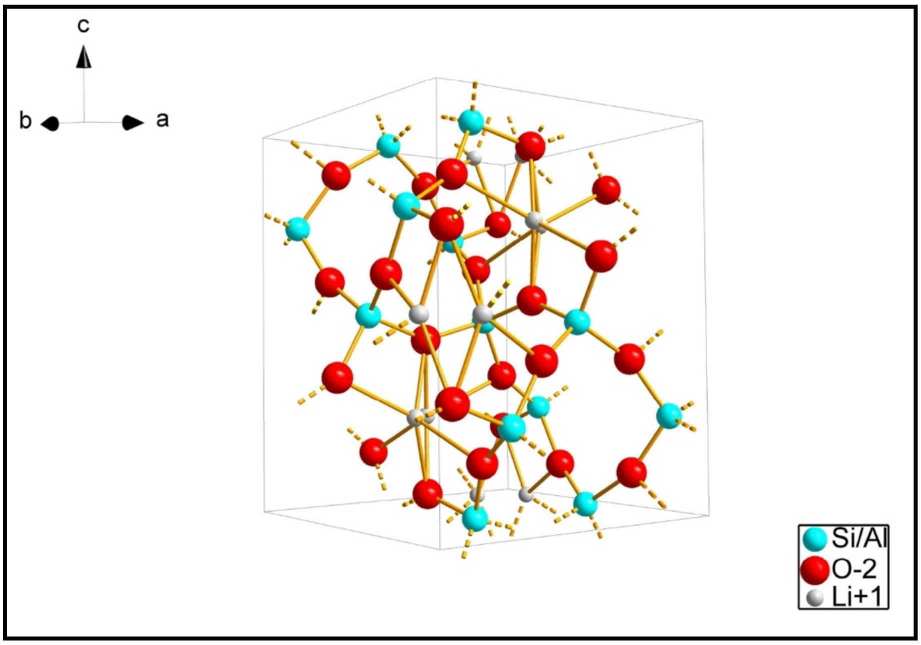

Figure 4: *Crystalline structure of β-spodumene (ICSD 26817) generated from the Diamond 4.6.3 software (Crystal Impact).*

Figure 5 presents the experimental XRPD's (Y_{obs}), the least-squares fit by the Rietveld refinement method (Y_{calc}), and the intensities difference (Y_{obs}- Y_{calc}) for the chromium-doped β-spodumene pigment samples produced. Table 01 presents the refinement quality factors, expressed as a percentage: permitted error (R_P), obtained error (R_{WP}) and expected error (R_E). The R_{WP}/R_E ratio, or simply χ, is of critical importance. If $\chi \cong 1$ indicates good quality refinement since $R_{WP} \cong R_E$ (only $\chi \geq 1$ values are possible) [24]. Integrated intensities R-factors (R_{Bragg}) are quoted as an indicator of the fit quality between observed and calculated [25].

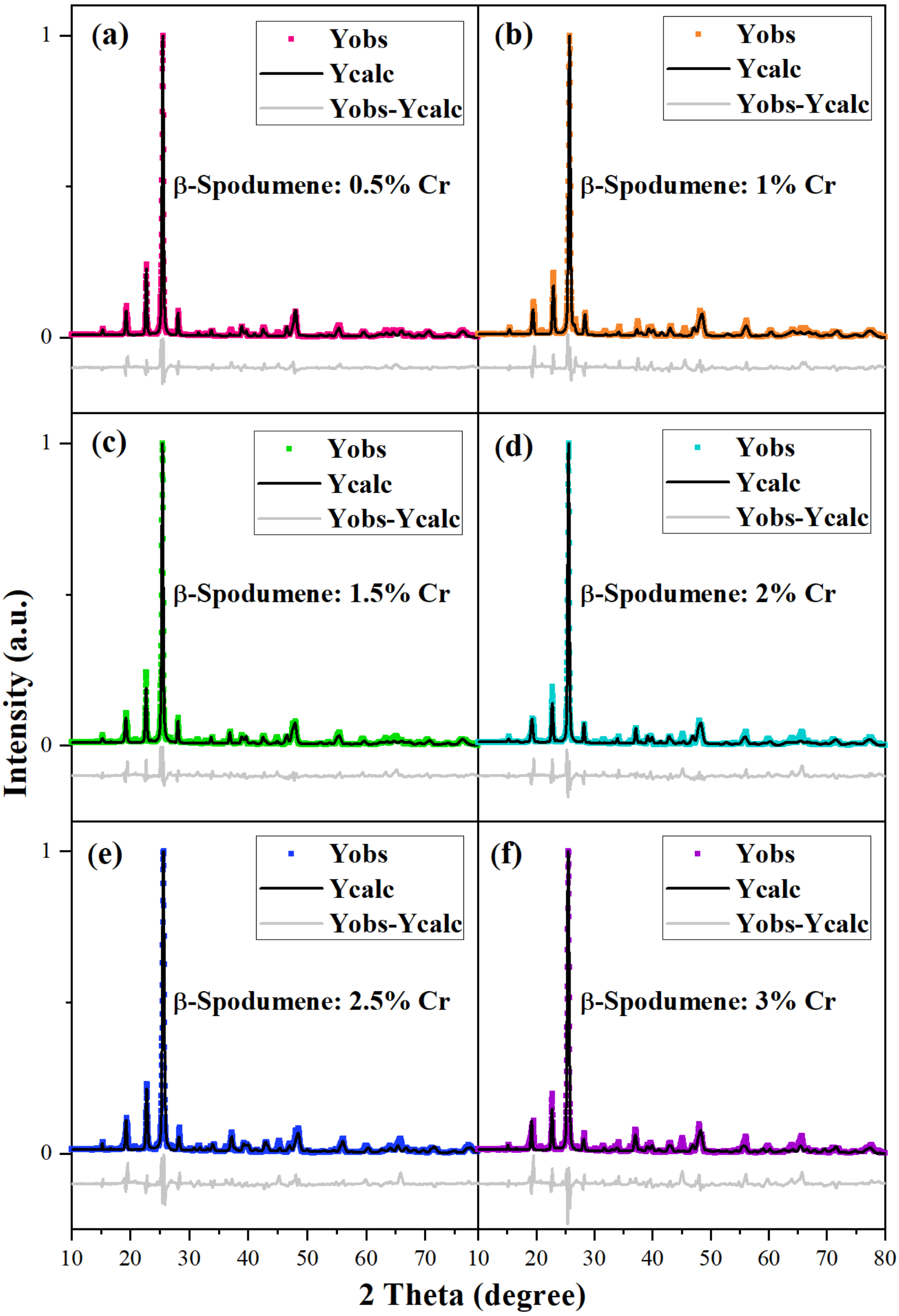

Figure 5: *Experimental XRPD's for different samples of chromium-doped β-spodumene pigment samples (Y_{obs}) and the fit calculated by the Rietveld method (Y_{calc}). The result of refinement is the intensities difference (Y_{obs}- Y_{calc}).*

Table 1: Quality factors of the Rietveld refinement fit of experimental XRPD's.

Sample	R_p (%)	R_{wp} (%)	R_e (%)	χ	R_{Bragg} (%)
β-Spodumene: 0.5% Cr	14.47	19.23	12.92	1.48	12.07
β-Spodumene: 1% Cr	15.68	21.47	12.98	1.65	11.95
β-Spodumene: 1.5% Cr	14.40	19.12	13.08	1.45	11.71
β-Spodumene: 2% Cr	16.90	22.82	13.35	1.70	13.96
β-Spodumene: 2.5% Cr	15.64	21.07	13.47	1.56	15.97
β-Spodumene: 3% Cr	19.77	26.00	13.64	1.90	22.61

The result of the Rietveld refinement provides a good fit, which is expressed as low χ values. This indicates few errors obtained in the process and demonstrates quantitatively that the experimental XRPD's correspond to the ICSD 26817 reference pattern of β-spodumene structure. The R_{Bragg} values obtained demonstrate that the 0.5 to 2.5% chromium-doped samples approximate 12 to 16% of the β-spodumene perfect structure. However, for the 3% chromium-doped sample, there is an increase in factors values to $\chi = 1.90$ and $R_{Bragg} = 22.6\%$ indicating a possible chromium saturation point. Despite this, no peaks corresponding to additional phases were identified.

Table 2 shows the average sizes of crystallites obtained by Scherrer's method. The values reveal that there is no tendency to reduce (or increase) the average size of crystallites with increasing dopant content. The values oscillate alternately, which shows a constant trend in this range. This indicates that the addition of chromium in the spodumene structure does not generate significant distortions in the crystal lattice, which is possibly due to the substitution of Al^{3+} for Cr^{3+}.

Table 2: Average crystallite size (Scherrer's method).

Sample	τ (nm)
β-Spodumene: 0.5% Cr	44.94 ± 0.05
β-Spodumene: 1% Cr	42.74 ± 0.05
β-Spodumene: 1.5% Cr	46.38 ± 0.05
β-Spodumene: 2% Cr	55.20 ± 0.05
β-Spodumene: 2.5% Cr	44.53 ± 0.05
β-Spodumene: 3% Cr	55.74 ± 0.05

It is known that Cr^{3+} ions occupy pseudo-octahedral sites in the spodumene clinopyroxene (monoclinic system) structure [26] and the substitution of Cr^{3+} ions has already been identified in Al^{3+} sites in natural spodumene (α-spodumene) using the Cr^{3+} luminescence technique [27]. Although spodumene crystallizes in the tetragonal system (β-spodumene) at high temperatures, the substitution in Al^{3+} sites is more probable, due to the same charge and the proximity of the ionic radius of these species.

The results presented demonstrate that the production of chromium-doped β-spodumene pigment samples by the proteic sol-gel route preserved the crystal structure of the pure material. Cr^{3+} ions can be incorporated into the structure by replacing Al^{3+} ions, which have similar chemical properties (charge and radius). Thus, no distortions were observed in the lattice, as well as the absence of a second phase formation in the samples produced. The preservation of the material's structure is a good indication that its chemical and thermal stabilities are preserved, which is of great importance for industrial ceramic pigments applications.

Although the β-spodumene ceramic is chemically inert and thermally stable, and the chromium dopant addition has not caused changes in the structure of the lattice, its application is recommended only in industrial applications, since studies on its toxicity have not been conducted. Its use as a biomaterial is not recommended while there are no studies on its biocompatibility. The chromium-doped β-spodumene based pigment has a great potential in the ceramic materials industry, and its performance can be tested on glasses, porcelains, refractories, among others.

3.2. Morphological characterization

Figure 6 illustrates the SEM micrographs for 0.5 (a), 1.5 (b) and 3.0% (c) chromium-doped β-spodumene pigment samples. Particles of micrometric order are presented, which have irregular and angular morphology, with a particle size in the range of 50 to 200 μm. These particles are polycrystalline, given the average size of the crystallites, which are of nanometric order. These crystallites have an organized structure of tetragonal cell repeats and are distributed in each particle in random orientations. In the 500x magnification micrographs, it is already possible to notice the presence of well-defined edges (highlighted in the figure). This type of particle morphology has already been identified for β-spodumene samples [28]. No change in the size or morphology of the particles was observed with the increase in the chromium content for the samples, which was expected since no structural changes were evidenced.

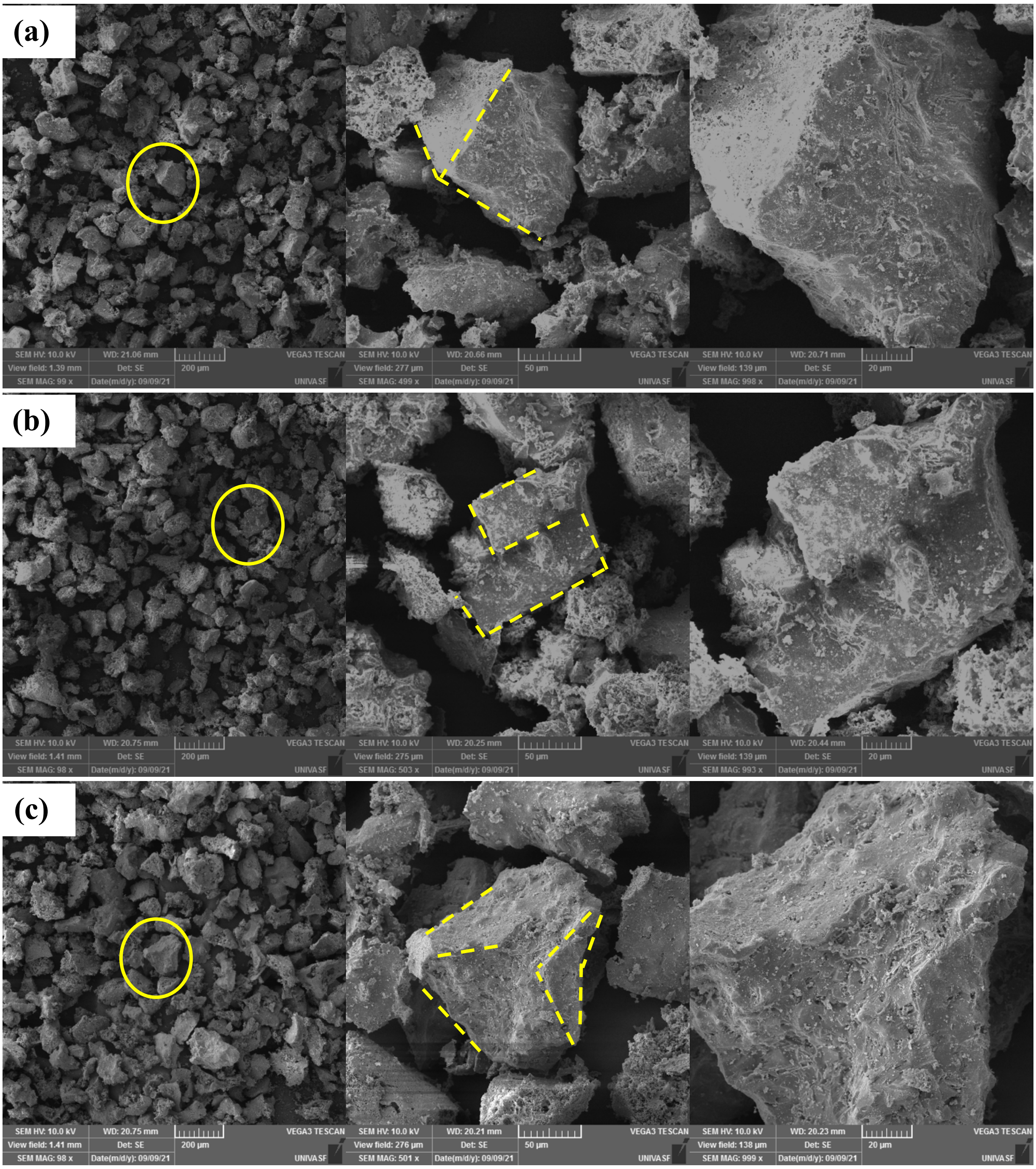

Figure 6: *SEM micrographs of the chromium doped β-spodumene pigment samples at 100, 500 and 1000x magnifications: (a) 0.5% Cr; (b) 1.5% Cr; (c) 3% Cr.*

In this analysis, samples obtained after the calcination process were used, without applying mechanical efforts or sieving, to preserve the morphology of the formed particles to be analyzed. However, for the application of ceramic pigments, processing (ball milling, or others) is indicated to reduce the particle size, increase the specific area, and improve their performance.

4. CONCLUSION

The present research investigates the structural and morphological properties of the chromium-doped β-spodumene based ceramic pigment, aiming to define whether this material preserves its chemical and thermal stability when modified with the addition of the doping chromophore metal. The material was synthesized by the proteic sol-gel method, using gelatin as a ligand, and doped with 0.5 to 3% of chromium, by weight.

XRD analysis confirmed the formation of the single-phase of β-spodumene for all samples doped with a concentration up to 3% by weight of chromium. Rietveld refinement presented well-adjusted fit factors and the absence of a second phase formation in the samples produced. Scherrer's method confirmed that there is no decreasing or increasing trend in the average size of nanometric crystallites with increasing chromium content. Also, no changes in the morphology or size of the particles were noted with the increase in the dopant content, from the SEM analysis.

The unaltered structural and morphological properties are an excellent indicator of the preservation of the chemical and thermal stability of β-spodumene, characteristics that are extremely relevant in the ceramic pigment industry. This can be explained by the replacement of Al^{3+} ions by Cr^{3+} in the β-spodumene matrix, when added at low doping contents, due to similar chemical properties, such as radius and charge.

ACKNOWLEDGMENT

The authors are thankful to the Brazilian Research Support Agencies: Coordenação de Aperfeiçoamento de Pessoal de Nível Superior - Brazil (CAPES) and Financiadora de Estudos e Projetos – FINEP (Chamada Pública MCTI/FINEP/FNDCT 02/2016, ref. 0533/16).

REFERENCES

[1] BARBOSA, L. I.; VALENTE, G.; OROSCO, R. P.; GONZÁLEZ, J. A. Lithium extraction from β-spodumene through chlorination with chlorine gas. **Minerals Engineering**, v. 56, p. 29-34, 2014.

[2] DESSEMOND, C; LAJOIE-LEROUX, F.; SOUCY, G.; LAROCHE, N.; MAGNAN, J. Spodumene: The Lithium Market, Resources and Processes. **Minerals**, v. 9(6), p. 334, 2019.

[3] KUANG, G.; LIU, Y.; LI, H.; XING, S.; LI, F.; GUO, H.; Extraction of lithium from β-spodumene using sodium sulfate solution. **Hydrometallurgy**, v. 177, p. 49-56, 2018.

[4] XING, P.; WANG, C.; MA, L. Z. B.; WANG, L.; CHEN, Y.; YANG, C. Lithium Extraction and Hydroxysodalite Zeolite Synthesis by Hydrothermal Conversion of α-Spodumene. **ACS Sustainable Chem Eng**, v. 7, p. 9498-9505, 2019.

[5] ROSALES, G. D.; RUIZ, M. C.; RODRIGUEZ, M. H. Novel process for the extraction of lithium from β-spodumene by leaching with HF. **Hydrometallurgy**, v. 147-148, p. 1-6, 2014.

[6] d'AMORIM, R. A. P. O.; TEIXEIRA, M. I.; SOUZA, S. O.; SASAKI, J. M.; CALDAS, L. V. E. Influence of Teflon® agglutinator on TLD spodumene pellets. **Journal of Luminescence**, v. 132, p. 266-269, 2012.

[7] d'AMORIM, R. A. P. O.; VASCONCELOS, D. A. A.; BARROS, V. S. M.; KHOURY, H. J.; SOUZA, S. O. Characterization of α-spodumene to OSL dosimetry. **Radiation Physics and Chemistry**, v. 95, p. 141-144, 2014.

[8] FERRAZ, G. M.; PAIÃO, J. R. B.; WATANABE, S.; SOUZA, S. O. Synthetic spodumene polycrystals as a TL dosimetric material. **Radiation Measurements**, v. 43, p. 387-391, 2008.

[9] LIMA, L. L.; OLIVEIRA, R. A. P.; LIMA, H. R. B. R.; SANTOS, H. N.; SANTOS, J. O.; LIMA, A. F.; SOUZA, S. O. Thermoluminescent properties studies of spodumene lilac sample to dosimetric applications. **Journal of Physics Conference Series**, v. 249(1), p. 012013, 2010.

[10] LIMA, H. R. B. R.; NASCIMENTO, D. S.; BISPO, G. F. C.; TEIXEIRA, V. C.; VALÉRIO, M. E. G.; SOUZA, S. O. Production and characterization of spodumene dosimetric pellets prepared by a sol–gel route. **Radiation Physics and Chemistry**, v. 104, p. 93-99, 2014.

[11] FERRAZ, R. F.; SOUSA, J. F.; COSTA, D. S.; OLIVEIRA, R. A. P.; LIMA, H. R. B. R. Development of a β-$LiAlSi_2O_6$:Cr-based Ceramic Pigment by Proteic Sol-Gel Process Using Gelatin: Synthesis and Characterization. **Materials Research**, v. 25(1), p. 12, 2022.

[12] BUXBAUM, G.; PFFAF, G. **Industrial Inorganic Pigments**, 3rd ed. Weinhein: WILEY-VCH Verlag GmbH & Co KGaA, 2005.

[13] MASLENNIKOVA, G. N.; PISHCH, I. V.; RADION, E. V. Current Classification of Ceramic Silicate Pigments (Review). **Glass and Ceramics**, v. 63, p. 281-284, 2006.

[14] ZHANG. A.; MU, B.; WANG, X.; WEN, L.; WANG, A. Formation and Coloring Mechanism of Typical Aluminosilicate Clay Minerals for $CoAl_2O_4$ Hybrid Pigment Preparation. **Frontiers in Chemistry**, v. 6, p. 125, 2018.

[15] GONG, L.; LIANG, J.; KONG, L.; CHEN, B.; LI, Y.; TIAN, G. Synthesis of high-performance copper barium silicate composite pigment from waste iron ore tailings. **Ceramics International**, v. 47(19), p. 27987-27997, 2021.

[16] KLEIN, L.; APARICIO, M.; JITIANU, A. **Handbook of Sol-Gel Science and Technology**, 2nd ed. New York: Springer, 2018.

[17] NOGUEIRA, N. A. S.; UTUNI, V. H. S.; SILVA, Y. C.; KIYOHARA, P. K.; VASCONCELOS, I. F.; MIRANDA, M. A. R.; SASAKI, J. M. X-ray diffraction and Mossbauer studies on superparamagnetic nickel ferrite ($NiFe_2O_4$) obtained by the proteic sol-gel method. **Materials Chemistry and Physics**, v. 163, p. 402-406, 2015.

[18] MENEZES, A. S.; REMÉDIOS, C. M. R.; SASAKI, J. M.; SILVA, L. R. D.; GOES, J. C.; JARDIM, P. M.; MIRANDA, M. A. R. Sintering of nanoparticles of α-Fe2O3 using gelatin. **J Non-Cryst Solids**, v. 353, p. 1091-1094, 2007.

[19] SCHIRIEBER, G.; GAREIS, H. **Gelatine Handbook: Theory and Industrial Practice**, 1st ed. Weinhein: WILEY-VCH Verlag GmbH & Co KGaA, 2007.

[20] RIETVELD, H. M. A profile refinement method for nuclear and magnetic structures. **J Appl Cryst**, v. 2, p. 65-71, 1969.

[21] BLEICHER, L.; SASAKI, J. M.; OLIVEIRA, C.; SANTOS, P. Development of a graphical interface of the Rietveld refinement program DBWS. **J Appl Cryst**, v. 33, p. 1189, 2000.

[22] SCHERRER, P.; Abschätzungen von Charaktersummen, Einheit und Klassenzahlen. **Göttinger Nachrichten Gesell**, v. 2, p. 98, 1918.

[23] CHI-TANG, L.; PEACOR, D. R.; The crystal structure of $LiAlSi_2O_6$-II (“β spodumene”). **Z Kristallogr**, v. 126, p. 46-65, 1968.

[24] YOUNG, R. A. Introduction to the Rietveld method. In: YOUNG, R. A. **The Rietveld Method**, 1st ed. New York: Oxford University Press, p. 1-38, 1993.

[25] DAVID, W. I. F.; Powder diffraction: least-squares and beyond. **J Res Natl Inst Stand Technol**, v. 109, p. 107-123, 2004.

[26] KHOMENKO, V. M.; PLATONOV, A. N. Electronic absorption spectra of Cr^{3+} ions in natural clinopyroxenes. **Phys Chem Minerals,** v. 11, p. 261-265, 1985.

[27] O’BANNON III, E.; WILLIAMS, Q. A Cr^{3+} luminescence study of spodumene at high pressures: Effects of site geometry, a phase transition, and a level-crossing. **American Mineralogist**, v. 101, p. 1406-1413, 2016.

[28] BARBOSA, L. I.; VALENTE, G.; OROSCO, R. P.; GONZÁLEZ, J. A. Lithium extraction from β-spodumene through chlorination with chlorine gas. **Miner Eng**, v. 56, p. 29-34, 2014.